INTERNATIONAL JOURNAL OF
NUMERICAL ANALYSIS AND MODELING
Volume 22, Number 3, Pages 432–458

doi: 10.4208/ijnam2025-1019

# A CONFORMING DISCONTINUOUS GALERKIN FINITE ELEMENT METHOD FOR SECOND-ORDER PARABOLIC EQUATION

FUCHANG HUO, YUCHEN SUN, JIAGENG WU, AND LIYUAN ZHANG*

**Abstract.** The conforming discontinuous Galerkin (CDG) finite element method is an innovative and effective numerical approach to solve partial differential equations. The CDG method is based on the weak Galerkin (WG) finite element method, and removes the stabilizer in the numerical scheme. And the CDG method uses the average of the interior function to replace the value of the boundary function in the standard WG method. The integration by parts is used to construct the discrete weak gradient operator in the CDG method. This paper uses the CDG method to solve the parabolic equation. Firstly, the semi-discrete and full-discrete numerical schemes of the parabolic equation and the well-posedness of the numerical methods are presented. Then, the corresponding error equations for both numerical schemes are established, and the optimal order error estimates of $H^1$ and $L^2$ are provided, respectively. Finally, the numerical results of the CDG method are verified.

**Key words.** Conforming discontinuous Galerkin finite element method, parabolic equation, weak Galerkin finite element method, optimal order convergence.

## 1. Introduction

The parabolic equation is an essential class of equations in partial differential equations. Its unique concept and properties make it play a huge role in physics and mathematics and have significant theoretical value. Many problems can be described by parabolic equations in life, for example, heat conduction of objects, flow problems of porous media, and diffusion problems of pollutant concentration. It is challenging to obtain analytical solutions on these practical problems, so scholars began to study their numerical solutions, which provides a solid theoretical basis for solving practical problems.

In this paper, we consider the initial-boundary value problems for second-order parabolic equation: Find $u$ satisfies

$$(1)\qquad \begin{cases} u_t - \nabla\cdot(a\nabla u) = f, & \mathbf{x}\in\Omega,\quad t\in J,\\ u = 0, & \mathbf{x}\in\partial\Omega,\ t\in J,\\ u(\cdot,0) = \psi, & \mathbf{x}\in\Omega,\end{cases}$$

where $J=\left[0,\overline{T}\right]$, $\overline{T}>0$, $\Omega\subset\mathbb{R}^2$ is a polygon domain, and the boundary $\partial\Omega$ is Lipschitz continuous. And the source term $f(x,t)\in L^\infty\Big(0,\overline{T};L^2(\Omega)\Big)$ and the initial value $\psi\in H^2(\Omega)$. Assume that $a(\cdot)_{2\times 2}\in[L^\infty(\Omega)]^{2\times 2}$ is a symmetric matrix-valued function, which satisfies

$$C_1\eta^T\eta\le\eta^T a\eta\le C_2\eta^T\eta,\quad \forall\eta\in\mathbb{R}^2,$$

here $C_1$ and $C_2$ are two positive constants with $0<C_1<C_2\ll\infty$.

Received by the editors on October 12, 2023 and, accepted on December 18, 2024.
2000 *Mathematics Subject Classification.* 65N30, 65N15, 65N12, 35K20, 35J50.
*Corresponding author.

The variational formulation of the parabolic equation (1) is to find $u \in L^2\Big(0, \overline{T}; [H_0^1(\Omega)]^d\Big)$, such that

$$\begin{cases} (u_t, v) + (a\nabla u, \nabla v) &= (f, v), \quad \forall\, v \in H_0^1(\Omega),\, t \in J, \\ u(\cdot, 0) &= \psi. \end{cases} \tag{2}$$

The Sobolev spaces are defined as follows:

$$H^1(\Omega) := \left\{ v | v \in L^2(\Omega), \nabla v \in [L^2(\Omega)]^2 \right\},$$

$$H_0^1(\Omega) := \left\{ v | v \in H^1(\Omega), v|_{\partial\Omega} = 0 \right\},$$

$$L^2(0, \overline{T}; V) := \left\{ v \,|\, v(\cdot, t) \in V, \, \forall t \in \left[0, \overline{T}\right], \int_0^{\overline{T}} \|v(\cdot, t)\|_V^2 dt < \infty \right\},$$

here $V$ is a Sobolev space with a norm $\|\cdot\|_V$.

There are many numerical methods to solve the parabolic equation, such as the finite element method (FEM) [14, 33], the nonconforming finite element method (NC-FEM) [31], the discontinuous Galerkin (DG) finite element method [3, 13], the virtual element method [15, 32], the weak Galerkin (WG) finite element method [1, 4, 5, 21], etc. In this paper, we propose a conforming discontinuous Galerkin (CDG) finite element method to solve the parabolic equation.

The CDG method is based on the WG method [2, 6, 7, 16, 17, 22]. Its main idea is to use the discontinuous polynomial as the approximate function and increase the degree of the polynomial for calculating the weak differential operators. Using higher-order degree polynomials can effectively ensure the weak continuity of discontinuous functions over element boundaries and substantially reduce computational complexity without altering the dimensions of the stiffness matrix and the global sparsity. In contrast to the WG method, the CDG method uses the averages of the interior functions to replace the boundary functions, reducing the number of boundary degrees of freedom. It has the advantages of being easy to construct the finite element space and the numerical scheme. In addition, the CDG numerical scheme is amenable to parallel computing, thereby effectively mitigating the computational overhead. Recently, the CDG method has garnered considerable scholarly attention and has been successfully used to solve the second-order elliptic problems [25–27], Stokes problems [10, 28], Biharmonic problems [29, 30], elliptic interface problems [23], linear elasticity interface problems [24], and so on.

In this paper, we use the CDG method to solve the initial-boundary value problems for second-order parabolic equation. In the CDG scheme, the approximation of the function is achieved through the employment of the discontinuous $k$-th degree polynomial. Concomitantly, the stabilizer terms within the numerical method are eliminated by increasing the polynomial degree for calculating the weak differential operators. The numerical schemes are presented for the semi-discrete spatial case, wherein only space is discretized, and the full-discrete case, which involves the discretization of time and space. Subsequently, the error equations for semi-discrete and full-discrete schemes are presented. Additionally, optimal order error estimates in the $H^1$ and $L^2$ norms are derived.

An outline of this paper is as follows. In Section 2, we propose a semi-discrete CDG scheme for the parabolic equation (1). In Section 3, the full-discrete CDG scheme for the parabolic equation (1) is established. In Section 4, we derive the optimal order error estimate for the semi-discrete CDG scheme and full-discrete CDG scheme. In Section 5, numerical results are presented to validate the accuracy and effectiveness of the CDG method. In Section 6, we provide a comprehensive summary of the content encapsulated within this paper.

## 2. Semi-discrete CDG scheme

In this section, we construct the semi-discrete CDG scheme for the parabolic equation (1) and study the stability of the semi-discrete CDG scheme.

Let $\mathcal{T}_h$ be the partition of $\Omega$ satisfying the shape regularity hypothesis [19, 20]. For each $T \in \mathcal{T}_h$, $h_T$ represents the diameter of $T$, $h = \max_{T\in\mathcal{T}_h} h_T$ represents the mesh size of $\mathcal{T}_h$. Let $\mathcal{E}_h$ be the set of all edges in $\mathcal{T}_h$ and $\mathcal{E}_h^0$ be the set of all interior edges in $\mathcal{T}_h$.

For any integer $k \geq 1$, we define the weak finite element space $V_h$ and the subspace $V_h^0$ as follows:

$$V_h = \{v \in L^2(\Omega), v|_T \in P_k(T), T \in \mathcal{T}_h\},$$
$$V_h^0 = \{v \in V_h, v = 0 \ on \ \partial\Omega\}.$$

Let $e \in \mathcal{E}_h$ be the shared edge of element $T_1$ and $T_2$. For any $v \in V_h + H_0^1(\Omega)$, the average $\{\cdot\}$ and jump $[\cdot]$ are defined by

$$\{v\} = \begin{cases} \frac{1}{2}v|_{T_1} + \frac{1}{2}v|_{T_2}, & e \in \mathcal{E}_h^0, \\ v, & e \in \partial\Omega, \end{cases} \tag{3}$$

and

$$[v] = \begin{cases} v|_{T_1} - v|_{T_2}, & e \in \mathcal{E}_h^0, \\ v, & e \in \partial\Omega. \end{cases} \tag{4}$$

According to the definitions of the average (3) and jump (4), it is easy to show that

$$\begin{cases} \|v - \{v\}\|_e = \dfrac{1}{2}\|[v]\|_e, & e \in \mathcal{E}_h^0, \\ \|v - \{v\}\|_e = 0, & e \in \partial\Omega. \end{cases} \tag{5}$$

Now, we define the discrete weak gradient operator.

**Definition 2.1.** *[18, 25] For any $v \in V_h + H^1(\Omega)$, its discrete weak gradient $\nabla_w v \in [P_j(T)]^2$ $(j > k)$ satisfies*

$$(\nabla_w v, \boldsymbol{\tau})_T = -(v, \nabla \cdot \boldsymbol{\tau})_T + \langle \{v\}, \boldsymbol{\tau} \cdot \mathbf{n}\rangle_{\partial T}, \quad \forall\, \boldsymbol{\tau} \in [P_j(T)]^2, \tag{6}$$

*where $\mathbf{n}$ is the unit outward normal direction on $\partial T$.*

Let $Q_h$ be the $L^2$ projection onto $P_k(T)$, $\mathbf{R}_h$ be the $L^2$ projection onto $[P_j(T)]^2$. For any $w, v \in V_h$, define

$$a(w, v) = \sum_{T\in T_h} (a\nabla_w w, \nabla_w v)_T.$$

**Semi-discrete CDG Algorithm 1.** *The semi-discrete CDG scheme of the parabolic equation (1) is given by seeking $u_h \in L^2(0, \overline{T}; V_h^0)$ and $u_h(\cdot, 0) = Q_h\psi$, such that*

$$((u_h)_t, v) + a(u_h, v) = (f, v), \quad \forall\, v \in V_h^0. \tag{7}$$

*Here $(u_h)_t$ represents the derivative of $u_h$ with respect to $t$.*

For any $v \in V_h + H^1(\Omega)$, we define two semi-norms as follows:

$$|\!|\!| v |\!|\!|^2 = \sum_{T\in T_h} (\nabla_w v, \nabla_w v)_T, \tag{8}$$

$$\|v\|_{1,h}^2 = \sum_{T\in T_h} \|\nabla v\|_T^2 + \sum_{e\in\varepsilon_h^0} h_e^{-1}\|[v]\|_e^2. \tag{9}$$

**Lemma 2.1.** *[25] For all $v \in V_h + H^1(\Omega)$, there exist two positive constants $C_1$ and $C_2$, such that*

$$C_1\|v\|_{1,h} \le |||v||| \le C_2\|v\|_{1,h}, \tag{10}$$

*which implies $j = n + k - 1$, where $n$ is the number of edges of convex polygon.*

From the the definition of $|||\cdot|||$ and Lemma 2.1, it is simple to get the following results.

**Lemma 2.2.** *$|||\cdot|||$ is a norm in $V_h^0$.*

**Lemma 2.3.** *[9] For any $w, v \in V_h$, there exist two positive constants $\alpha, \beta$, such that*

$$|a(w,v)| \le \beta|||w||| |||v|||, \tag{11}$$

$$\alpha|||v|||^2 \le a(v,v). \tag{12}$$

For the semi-discrete CDG scheme (7), we have the following stable result.

**Theorem 2.1.** *Let $u_h(t) \in L^2(0,\overline{T}; V_h^0)$ be the numerical solution of the semi-discrete CDG scheme (7), there exists $C > 0$ such that*

$$\|u_h(t)\|^2 \le C\left(\|u_h(0)\|^2 + \int_0^t \|f(s)\|^2 ds\right), \forall\, t \in (0,\overline{T}], \tag{13}$$

*where $C$ is independent of $h$ and $t$.*

*Proof.* By setting $v = u_h$ in (7), we have

$$((u_h(t))_t, u_h(t)) + a(u_h(t), u_h(t)) = (f, u_h(t)).$$

From the coercive of the bilinear form $a(\cdot,\cdot)$ in (12), we get

$$(f, u_h(t)) \ge ((u_h(t))_t, u_h(t)),$$

which yields

$$\int_\Omega f\, u_h(t)dx \ge ((u_h(t))_t, u_h(t)) = \frac{1}{2}\frac{d}{dt}\int_\Omega u_h^2(t)dx.$$

By using the Young inequality, we obtain

$$\frac{1}{2}\frac{d}{dt}\int_\Omega u_h^2(t)dx \le \frac{1}{2}\left(\int_\Omega f^2 dx + \int_\Omega u_h^2(t)dx\right).$$

By integrating the above equation with respect to $t$, we arrive at

$$\|u_h(t)\|^2 \le \|u_h(0)\|^2 + \int_0^t \|f(s)\|^2 ds + \int_0^t \|u_h(s)\|^2 ds. \tag{14}$$

Combining (14) and Gronwall inequality [12] yield (13). The proof is completed. □

Now, we give some results about the projection operator $Q_h$ and $\mathbf{R}_h$. Recall the definitions of projection operator, denote by $Q_h$ the $L^2$ projection operator onto $P_k(T)$ and by $\mathbf{R}_h$ the $L^2$ projection operator onto $[P_{n+k-1}(T)]^2$.

**Lemma 2.4.** *[18] For any $\varphi \in H^{k+1}(\Omega)$, there hold*

$$\sum_{T\in\mathcal{T}_h} \|\varphi - Q_h\varphi\|_T^2 + \sum_{T\in\mathcal{T}_h} h_T^2 \|\nabla(\varphi - Q_h\varphi)\|_T^2 \le Ch^{2(k+1)}\|\varphi\|_{k+1}^2, \tag{15}$$

$$\sum_{T\in\mathcal{T}_h} \|a(\nabla\varphi - \mathbf{R}_h(\nabla\varphi))\|_T^2 \le Ch^{2k}\|\varphi\|_{k+1}^2. \tag{16}$$

**Lemma 2.5.** *For $u \in H^1(\Omega)$, we have*

$$\nabla_w u = \mathbf{R}_h \nabla u. \tag{17}$$

*Proof.* From the definition of the weak gradient (6), integration by parts, and the definition of $\mathbf{R}_h$, we get

$$\begin{aligned}(\nabla_w u, \boldsymbol{\tau})_T &= -(\nabla\cdot\boldsymbol{\tau}, u)_T + \langle\{u\}, \boldsymbol{\tau}\cdot\mathbf{n}\rangle_{\partial T}\\ &= -(\nabla\cdot\boldsymbol{\tau}, u)_T + \langle u, \boldsymbol{\tau}\cdot\mathbf{n}\rangle_{\partial T}\\ &= (\nabla u, \boldsymbol{\tau})_T - \langle u, \boldsymbol{\tau}\cdot\mathbf{n}\rangle_{\partial T} + \langle u, \boldsymbol{\tau}\cdot\mathbf{n}\rangle_{\partial T}\\ &= (\mathbf{R}_h\nabla u, \boldsymbol{\tau})_T, \quad \forall\, \boldsymbol{\tau} \in [P_{n+k-1}(T)]^2,\end{aligned}$$

which proves (17). □

**Lemma 2.6.** *Let $u \in H^1(\Omega)$, there holds true*

$$(a\nabla_w u, \nabla_w v)_T = (\nabla v, a\nabla u)_T - \langle v - \{v\}, a\mathbf{R}_h\nabla u\cdot\boldsymbol{n}\rangle_{\partial T}, \quad \forall\, v \in V_h^0. \tag{18}$$

*Proof.* According to (17), integration by parts, and the definition of the weak gradient (6), we have

$$\begin{aligned}(a\nabla_w u, \nabla_w v)_T &= (a\mathbf{R}_h\nabla u, \nabla_w v)_T\\ &= -(v, \nabla\cdot(a\mathbf{R}_h\nabla u))_T + \langle\{v\}, (a\mathbf{R}_h\nabla u)\cdot\mathbf{n}\rangle_{\partial T}\\ &= (\nabla v, a\mathbf{R}_h\nabla u)_T - \langle v, a\mathbf{R}_h\nabla u\cdot\mathbf{n}\rangle_{\partial T} + \langle\{v\}, (a\mathbf{R}_h\nabla u)\cdot\mathbf{n}\rangle_{\partial T}\\ &= (\nabla v, a\nabla u)_T - \langle v - \{v\}, a\mathbf{R}_h\nabla u\cdot\mathbf{n}\rangle_{\partial T}.\end{aligned}$$

The proof is completed. □

Let $u$ be the exact solution of the parabolic equation (1), $u_h(t) \in L^2(0, \overline{T}; V_h^0)$ be the numerical solution of the semi-discrete CDG scheme (7), we define the error as follows:

$$e := u - u_h.$$

**Theorem 2.2.** *Assume $u \in C^1\left(0, \overline{T}; H^{k+1}(\Omega)\right)$, there exists a constant $C > 0$, such that*

$$\|e(\cdot,t)\|^2 + \int_0^t \alpha |\!|\!| e |\!|\!|^2 ds \le \|e(\cdot,0)\|^2 + Ch^{2k}\int_0^t \|u\|_{k+1}^2 ds, \tag{19}$$

*and*

$$\begin{aligned}\|e\|^2 + \int_0^t \|e_s\|^2 ds + \frac{\alpha}{4}|\!|\!| e |\!|\!|^2 \le &\|e(\cdot,0)\|^2 + \beta|\!|\!| e(\cdot,0) |\!|\!|^2 + Ch^{2k}\Big(\|u(\cdot,0)\|_{k+1}^2\\ &+ \|u\|_{k+1}^2 + \int_0^t \|u\|_{k+1}^2 ds + \|u_s\|_{k+1}^2 ds\Big).\end{aligned} \tag{20}$$

*Proof.* By testing (1) with $v \in V_h^0$, we have

$$(f, v) = (u_t, v) + \sum_{T\in\mathcal{T}_h} \left(-\nabla\cdot(a\nabla u), v\right)_T.$$

Using integration by parts, the fact that $\sum_{T\in\mathcal{T}_h}\langle a\nabla u\cdot\mathbf{n},\{v\}\rangle_{\partial T}=0$ and (18), we obtain

$$
\begin{aligned}
(f,v) =&(u_t,v)+\sum_{T\in\mathcal{T}_h}(-\nabla\cdot a\nabla u,v)_T\\
=&(u_t,v)+\sum_{T\in\mathcal{T}_h}(a\nabla u,\nabla v)_T-\sum_{T\in\mathcal{T}_h}\langle v,a\nabla u\cdot\mathbf{n}\rangle_{\partial T}\\
=&(u_t,v)+\sum_{T\in\mathcal{T}_h}(a\nabla u,\nabla v)_T-\sum_{T\in\mathcal{T}_h}\langle v-\{v\},a\nabla u\cdot\mathbf{n}\rangle_{\partial T}\\
=&(u_t,v)+\sum_{T\in\mathcal{T}_h}(a\nabla_w u,\nabla_w v)_T+\sum_{T\in\mathcal{T}_h}\langle v-\{v\},a\mathbf{R}_h\nabla u\cdot\mathbf{n}\rangle_{\partial T}\\
&-\sum_{T\in\mathcal{T}_h}\langle v-\{v\},a\nabla u\cdot\mathbf{n}\rangle_{\partial T}\\
=&(u_t,v)+\sum_{T\in\mathcal{T}_h}(a\nabla_w u,\nabla_w v)_T+\sum_{T\in\mathcal{T}_h}\langle a(\mathbf{R}_h\nabla u-\nabla u)\cdot\mathbf{n},v-\{v\}\rangle_{\partial T}.
\end{aligned}\tag{21}
$$

Subtracting (7) from (21), we arrive at

$$((u-u_h)_t,v)+\sum_{T\in\mathcal{T}_h}(a\nabla_w(u-u_h),\nabla_w v)_T=\sum_{T\in\mathcal{T}_h}\langle a(\nabla u-\mathbf{R}_h\nabla u)\cdot\mathbf{n},v-\{v\}\rangle_{\partial T},$$

which implies that

$$(e_t,v)+\sum_{T\in\mathcal{T}_h}(a\nabla_w e,\nabla_w v)_T=\sum_{T\in\mathcal{T}_h}\langle a(\nabla u-\mathbf{R}_h\nabla u)\cdot\mathbf{n},v-\{v\}\rangle_{\partial T}.\tag{22}$$

Using the Cauchy-Schwarz inequality, the trace inequality, and the Young inequality, we get

$$
\begin{aligned}
&\left|\sum_{T\in\mathcal{T}_h}\langle a(\nabla u-\mathbf{R}_h\nabla u)\cdot\mathbf{n},v-\{v\}\rangle_{\partial T}\right|\\
\le&\left(\sum_{T\in\mathcal{T}_h}h_T\|a(\nabla u-\mathbf{R}_h\nabla u)\|_{\partial T}^2\right)^{\frac12}\left(\sum_{T\in\mathcal{T}_h}h_T^{-1}\|v-\{v\}\|_{\partial T}^2\right)^{\frac12}\\
\le&C\left(\sum_{T\in\mathcal{T}_h}\left(\|a\left(\nabla u-\mathbf{R}_h\nabla u\right)\|_T^2+h_T^2\|\nabla(a(\nabla u-\mathbf{R}_h\nabla u))\|_T^2\right)\right)^{\frac12}\cdot|\!|\!|v|\!|\!|\\
\le&Ch^k\|u\|_{k+1}\cdot|\!|\!|v|\!|\!|\\
\le&Ch^{2k}\|u\|_{k+1}^2+\frac{\alpha}{2}|\!|\!|v|\!|\!|^2.
\end{aligned}\tag{23}
$$

By taking $v=e$ in (22), we have

$$(e_t,e)+\sum_{T\in\mathcal{T}_h}(a\nabla_w e,\nabla_w e)=\sum_{T\in\mathcal{T}_h}\langle a(\nabla u-\mathbf{R}_h\nabla u)\cdot\mathbf{n},e-\{e\}\rangle_{\partial T}.\tag{24}$$

According to the coercive of the bilinear form $a(\cdot,\cdot)$ in (12) and estimate (23), we obtain

$$\frac12\frac{d}{dt}\|e\|^2+\alpha|\!|\!|e|\!|\!|^2\le(e_t,e)+a(e,e)\le Ch^{2k}\|u\|_{k+1}^2+\frac{\alpha}{2}|\!|\!|e|\!|\!|^2,$$

which leads to

$$\frac{d}{dt}\|e\|^2+\alpha|\!|\!|e|\!|\!|^2\le Ch^{2k}\|u\|_{k+1}^2.\tag{25}$$

By integrating the above equation with respect to $t$, we arrive at

$$\|e\|^2 - \|e(\cdot,0)\|^2 + \alpha \int_0^t {|\!|\!|e|\!|\!|}^2 ds \le Ch^{2k} \int_0^t \|u\|_{k+1}^2 ds,$$

which yields

$$\|e\|^2 + \int_0^t \alpha {|\!|\!|e|\!|\!|}^2 ds \le \|e(\cdot,0)\|^2 + Ch^{2k} \int_0^t \|u\|_{k+1}^2 ds. \tag{26}$$

Then, we turn to estimate (20). Setting $v = e_t$ in (22), we get

$$\begin{aligned}
&(e_t, e_t) + (a\nabla_w e, \nabla_w e_t) \\
=& \sum_{T\in\mathcal{T}_h} \langle a(\nabla u - \mathbf{R}_h \nabla u)\cdot \mathbf{n}, e_t - \{e_t\}\rangle_{\partial T} \\
=& \frac{d}{dt} \sum_{T\in\mathcal{T}_h} \langle a(\nabla u - \mathbf{R}_h \nabla u)\cdot \mathbf{n}, e - \{e\}\rangle_{\partial T} - \sum_{T\in\mathcal{T}_h} \langle a(\nabla u_t - \mathbf{R}_h \nabla u_t)\cdot \mathbf{n}, e - \{e\}\rangle_{\partial T}.
\end{aligned}$$

By using the Cauchy-Schwarz inequality and the Young inequality, we have

$$\begin{aligned}
&\|e_t\|^2 + \frac{1}{2}\frac{d}{dt} a(e,e) \\
\le& \frac{d}{dt} \sum_{T\in\mathcal{T}_h} \langle a(\nabla u - \mathbf{R}_h \nabla u)\cdot \mathbf{n}, e - \{e\}\rangle_{\partial T} \\
&+ \left| \sum_{T\in\mathcal{T}_h} \langle a(\nabla u_t - \mathbf{R}_h \nabla u_t)\cdot \mathbf{n}, e - \{e\}\rangle_{\partial T} \right| \\
\le& \frac{d}{dt} \sum_{T\in\mathcal{T}_h} \langle a(\nabla u - \mathbf{R}_h \nabla u)\cdot \mathbf{n}, e - \{e\}\rangle_{\partial T} \\
&+ \frac{1}{4\alpha} \sum_{T\in\mathcal{T}_h} h_T \|a(\nabla u_t - \mathbf{R}_h \nabla u_t)\|_{\partial T}^2 + \alpha {|\!|\!|e|\!|\!|}^2.
\end{aligned} \tag{27}$$

Integrating the above equation with respect to $t$ and together with the bounded-ness (11), the Cauchy-Schwarz inequality, and the Young inequality, we get

$$\begin{aligned}
\int_0^t \|e_s\|^2 ds + \frac{\alpha}{2} {|\!|\!|e|\!|\!|}^2 \le& \frac{\beta}{2} {|\!|\!|e(\cdot,0)|\!|\!|}^2 + \sum_{T\in\mathcal{T}_h} \langle a(\nabla u - \mathbf{R}_h \nabla u)\cdot \mathbf{n}, e - \{e\}\rangle_{\partial T} \\
&- \sum_{T\in\mathcal{T}_h} \langle a\left(\nabla u(\cdot,0) - \mathbf{R}_h \nabla u(\cdot,0)\right)\cdot \mathbf{n}, e(\cdot,0) - \{e(\cdot,0)\}\rangle_{\partial T} \\
&+ \int_0^t \frac{1}{4\alpha} \left( \sum_{T\in\mathcal{T}_h} h_T \|a(\nabla u_s - \mathbf{R}_h \nabla u_s)\|_{\partial T}^2 \right) ds + \alpha \int_0^t {|\!|\!|e|\!|\!|}^2 ds \\
\le& \frac{\beta}{2} {|\!|\!|e(\cdot,0)|\!|\!|}^2 + \frac{1}{\alpha} \sum_{T\in\mathcal{T}_h} h_T \|a(\nabla u - \mathbf{R}_h \nabla u)\|_{\partial T}^2 + \frac{\alpha}{4} {|\!|\!|e|\!|\!|}^2 \\
&+ \frac{1}{2\beta} \sum_{T\in\mathcal{T}_h} h_T \|a\left(\nabla u(\cdot,0) - \mathbf{R}_h \nabla u(\cdot,0)\right)\|_{\partial T}^2 + \frac{\beta}{2} {|\!|\!|e(\cdot,0)|\!|\!|}^2 \\
&+ \int_0^t \frac{1}{4\alpha} \left( \sum_{T\in\mathcal{T}_h} h_T \|a(\nabla u_s - \mathbf{R}_h \nabla u_s)\|_{\partial T}^2 \right) ds + \int_0^t \alpha {|\!|\!|e|\!|\!|}^2 ds,
\end{aligned} \tag{28}$$

which yields

$$\begin{aligned}&\|e\|^2+\int_0^t\|e_s\|^2ds+\frac{\alpha}{4}|||e|||^2\\ \le&\|e(\cdot,0)\|^2+\beta|||e(\cdot,0)|||^2\\ &+Ch^{2k}\left(\|u(\cdot,0)\|_{k+1}^2+\|u\|_{k+1}^2+\int_0^t\|u\|_{k+1}^2ds+\int_0^t\|u_s\|_{k+1}^2ds\right).\end{aligned}$$

This completes the proof of the theorem. □

## 3. Full-discrete CDG scheme

This section is devoted to derive the full-discrete CDG scheme for the parabolic equation (1).

Let $\tau>0$ be the time step, we define $t_n=n\tau$, $0\le n\le N$, and $\tau=\overline{T}/N$. Besides, we introduce the backward Euler scheme as follows:

$$\overline{\partial}v^n=\frac{1}{\tau}(v^n-v^{n-1}),\tag{29}$$

where $v^n=v(t_n)$.

Letting $U^n:=u_h(t_n)\in V_h^0$ and applying the backward Euler difference scheme for time $t$ in the semi-discrete method, we obtain the following full-discrete CDG scheme.

**Full-Discrete CDG Algorithm 1.** *The full-discrete CDG scheme for the parabolic equation (1) is given by: Seeking $U^n\in V_h^0\,(n=1,2,\cdots,N)$ and $U^0=Q_h\psi$, such that*

$$(\overline{\partial}U^n,v)+a(U^n,v)=(f(t_n),v),\quad\forall\,v\in V_h^0.\tag{30}$$

From the (30) and (29), it is easy to get the following equivalent scheme.

**Full-Discrete CDG Algorithm 2.** *An equivalent full-discrete CDG scheme: Find $U^n\in V_h^0\,(n=1,2,\cdots,N)$ and $U^0=Q_h\psi$, such that*

$$(U^n,v)+\tau a(U^n,v)=(U^{n-1}+\tau f(t_n),v),\quad\forall\,v\in V_h^0.\tag{31}$$

**Theorem 3.1.** *The full-discrete CDG scheme (30) only has a unique solution.*

*Proof.* Let $U_{(1)}^n$ and $U_{(2)}^n$ be the two solutions of the full-discrete CDG scheme (30), satisfying $U_{(1)}^0=U_{(2)}^0=Q_h\psi$ and

$$(\overline{\partial}U_{(i)}^n,v)+a(U_{(i)}^n,v)=(f(t_n),v),\ i=1,2;\,\forall\,v\in V_h^0.$$

Letting $E^n=U_{(1)}^n-U_{(2)}^n$, it follows that $E^n\in V_h^0\,(E^0=0)$ and

$$(\overline{\partial}E^n,v)+a(E^n,v)=0,\quad\forall\,v\in V_h^0,\tag{32}$$

By taking $v=E^n$ in (32), we have

$$(\overline{\partial}E^n,E^n)+a(E^n,E^n)=0.\tag{33}$$

Using (29), we get

$$\begin{aligned}(\overline{\partial}E^n,E^n)&=\frac{1}{\tau}\left(E^n-E^{n-1},E^n\right)\\ &=\frac{1}{2\tau}\left((E^n,E^n)-(E^{n-1},E^{n-1})+(E^n-E^{n-1},E^n-E^{n-1})\right)\\ &\ge\frac{1}{2\tau}\left(\|E^n\|^2-\|E^{n-1}\|^2\right).\end{aligned}\tag{34}$$

Substituting (34) into (33) yields

$$\frac{1}{2\tau}\left(\|E^n\|^2-\|E^{n-1}\|^2\right)+\alpha|||E^n|||^2\le 0. \tag{35}$$

By induction yields

$$\|E^n\|^2+2\tau\alpha\sum_{j=1}^{n}|||E^j|||^2\le 0,$$

which implies that $|||E^j|||=0\,(1\le j\le n)$. From the definition of $|||\cdot|||$, we arrive at

$$E^j=0,\quad 1\le j\le n,$$

which yields

$$U^n_{(1)}=U^n_{(2)}.$$

The proof is completed. □

**Lemma 3.1.** *[9, 11] For all $v\in V_h^0$, there holds*

$$\|v\|^2\le C|||v|||^2. \tag{36}$$

For the full-discrete CDG scheme (30), it is simple to get the following stabilized conclusion.

**Theorem 3.2.** *Let $U^n$ be the numerical solution of the full-discrete CDG scheme (30) and assume $\|f(t)\|$ is bound in $J=\left[0,\overline{T}\right]$. Then, there holds*

$$\|U^n\|\le\|U^0\|+C\sup_{t\in\left[0,\overline{T}\right]}\|f(t)\|. \tag{37}$$

*Proof.* By setting $v=U^n$ in (30), together with the Young inequality, (12) and (36), we have

$$\begin{aligned}&\frac{1}{2}\|U^n\|^2-\frac{1}{2}\|U^{n-1}\|^2+\frac{1}{2}\|U^n-U^{n-1}\|^2+\alpha\tau|||U^n|||^2\\ \le&\tau(f(t_n),U^n)\\ \le&\frac{\tau}{\alpha}\|f(t_n)\|^2+\frac{\tau\alpha}{4}|||U^n|||^2,\end{aligned}$$

which yields

$$\|U^n\|^2\le\|U^{n-1}\|^2+C\tau\|f(t_n)\|^2.$$

Summing the above inequality from 1 to $n$, we get

$$\begin{aligned}\|U^n\|^2&\le\|U^0\|^2+C\tau\sum_{j=1}^{n}\|f(t_j)\|^2\\ &\le\|U^0\|^2+CT\sup_{t\in\left[0,\overline{T}\right]}\|f(t)\|^2.\end{aligned}$$

This completes the proof of the theorem. □

Denote by $e^n:=U^n-u(t_n)$ be the error of the full-discrete CDG scheme (30). We have the following error estimate results.

**Theorem 3.3.** *Suppose that $u\in C^2(0,\overline{T};H^{k+1}(\Omega))$, there hold*

$$\|e^n\|^2+\sum_{j=1}^{n}\alpha\tau|||e^j|||^2\le\|e^0\|^2+C\left(h^{2k}\|u\|^2_{k+1,\infty}+\tau^2\int_0^{t_n}\|u_{ss}\|^2ds\right), \tag{38}$$

*and*

$$\|\!|e^n|\!\|^2 \le C\Big\{\|e^0\|^2 + |\!\|e^0|\!\|^2 + h^{2k}\Big(\|u(\cdot,0)\|_{k+1}^2 + \|u\|_{k+1,\infty}^2 + \|u_t\|_{k+1,\infty}^2 + \tau^2\int_0^{t_n}\|u_{ss}\|_{k+1}^2 ds\Big) + \tau^2\int_0^{t_n}\|u_{ss}\|^2 ds\Big\}, \tag{39}$$

*where* $\|u\|_{k+1,\infty} = \sup_{t\in[0,T]} \|u(t)\|_{k+1}$.

*Proof.* For any $v \in V_h^0$, we have

$$(f(t_n), v) = (u_t(t_n), v) + \sum_{T\in\mathcal{T}_h} (a\nabla_w u(t_n), \nabla_w v)_T + \sum_{T\in\mathcal{T}_h} \langle a\,(\mathbf{R}_h\nabla u(t_n) - \nabla u(t_n))\cdot\mathbf{n}, v - \{v\}\rangle_{\partial T}. \tag{40}$$

From the full-discrete CDG scheme (30), we obtain

$$\left(\overline{\partial}U^n, v\right) + a\,(U^n, v) = (f(t_n), v)\,,\ \ \forall\, v \in V_h^0.$$

Subtracting the two equations yields

$$\left(\overline{\partial}U^n - u_t(t_n), v\right) + a(U^n - u(t_n), v) = \sum_{T\in\mathcal{T}_h} \langle a(\mathbf{R}_h\nabla u(t_n) - \nabla u(t_n))\cdot\mathbf{n}, v - \{v\}\rangle_{\partial T}\,, \tag{41}$$

From (29), it follows that

$$\left(\overline{\partial}U^n - u_t(t_n), v\right) = \left(\overline{\partial}(U^n - u(t_n)), v\right) + \left(\overline{\partial}u(t_n) - u_t(t_n), v\right). \tag{42}$$

Substituting (42) into (41) yields

$$\begin{aligned}&\left(\overline{\partial}(U^n - u(t_n)), v\right) + a\,(U^n - u(t_n), v)\\ =& \left(u_t(t_n) - \overline{\partial}u(t_n), v\right) - \sum_{T\in\mathcal{T}_h} \langle a(\nabla u(t_n) - \mathbf{R}_h\nabla u(t_n))\cdot\mathbf{n}, v - \{v\}\rangle_{\partial T},\end{aligned} \tag{43}$$

which leads to

$$\begin{aligned}&\left(\overline{\partial}e^n, v\right) + a(e^n, v)\\ =& \left(u_t(t_n) - \overline{\partial}u(t_n), v\right) - \sum_{T\in\mathcal{T}_h} \langle a(\nabla u(t_n) - \mathbf{R}_h\nabla u(t_n))\cdot\mathbf{n}, v - \{v\}\rangle_{\partial T}.\end{aligned} \tag{44}$$

For the convenience of description, we define the following notations:

$$\begin{aligned}\mathbb{W}_1^n &= u_t(t_n) - \overline{\partial}u(t_n),\\ \mathbb{W}_{2,T}^n &= (a\,(\nabla u(t_n) - \mathbf{R}_h\nabla u(t_n))\cdot\mathbf{n})\,|_{\partial T},\\ e_T^n &= (e(t_n) - \{e(t_n)\})\,|_{\partial T}.\end{aligned}$$

Taking $v = e^n$ in (44), we have

$$\left(\overline{\partial}e^n, e^n\right) + a(e^n, e^n) = (\mathbb{W}_1^n, e^n) - \sum_{T\in\mathcal{T}_h} \langle \mathbb{W}_{2,T}^n, e_T^n\rangle_{\partial T}.$$

By using (12), the Cauchy-Schwarz inequality, and the Young inequality, we get

(45)
$$\|e^n\|^2+\alpha\tau|\!|\!|e^n|\!|\!|^2 \le (e^{n-1},e^n)+\tau\|\mathbb{W}_1^n\|\cdot\|e^n\|+\tau\left|\sum_{T\in\mathcal{T}_h}\langle\mathbb{W}_{2,T}^n,e_T^n\rangle_{\partial T}\right|$$
$$\le \frac{1}{2}\|e^{n-1}\|^2+\frac{1}{2}\|e^n\|^2+\tau\|\mathbb{W}_1^n\|\cdot\|e^n\|+\tau\left|\sum_{T\in\mathcal{T}_h}\langle\mathbb{W}_{2,T}^n,e_T^n\rangle_{\partial T}\right|.$$

From (36), it follows that
$$\frac{1}{2}\|e^n\|^2+\alpha\tau|\!|\!|e^n|\!|\!|^2 \le \frac{1}{2}\|e^{n-1}\|^2+\frac{\tau\alpha}{4}|\!|\!|e^n|\!|\!|^2+\frac{\tau}{\alpha}\|\mathbb{W}_1^n\|^2 + \frac{\tau}{\alpha}\sum_{T\in\mathcal{T}_h}h_T\|a\left(\nabla u(t_n)-\mathbf{R}_h\nabla u(t_n)\right)\|_{\partial T}^2+\frac{\tau\alpha}{4}|\!|\!|e^n|\!|\!|^2,$$
which implies that

(46)
$$\frac{1}{2}\|e^n\|^2+\frac{1}{2}\alpha\tau|\!|\!|e^n|\!|\!|^2 \le\frac{1}{2}\|e^{n-1}\|^2+\frac{\tau}{\alpha}\|\mathbb{W}_1^n\|^2+\frac{\tau}{\alpha}\sum_{T\in\mathcal{T}_h}h_T\|a(\mathbf{R}_h\nabla u(t_n)-\nabla u(t_n))\|_{\partial T}^2.$$

Summing the above inequality from 1 to $n$, we have

(47)
$$\|e^n\|^2+\sum_{j=1}^n\alpha\tau|\!|\!|e^j|\!|\!|^2 \le\|e^0\|^2+\frac{2\tau}{\alpha}\sum_{j=1}^n\|\mathbb{W}_1^j\|^2+\frac{2\tau}{\alpha}\sum_{j=1}^n\sum_{T\in\mathcal{T}_h}h_T\|a(\nabla u(t_j)-\mathbf{R}_h\nabla u(t_j))\|_{\partial T}^2.$$

Noting that
$$\begin{aligned}\frac{1}{\tau}\int_{t_{j-1}}^{t_j}(s-t_{j-1})u_{ss}ds &= \frac{1}{\tau}\int_{t_{j-1}}^{t_j}(s-t_{j-1})du_s\\ &=\frac{1}{\tau}\left[(s-t_{j-1})u_t\Big|_{t_{j-1}}^{t_j}-\int_{t_{j-1}}^{t_j}u_sds\right]\\ &=\frac{1}{\tau}\Big[(t_j-t_{j-1})u_t(t_j)-(u(t_j)-u(t_{j-1}))\Big]\\ &=u_t(t_j)-\frac{u(t_j)-u(t_{j-1})}{\tau},\end{aligned}$$
then we get
$$\mathbb{W}_1^j=u_t(t_j)-\frac{u(t_j)-u(t_{j-1})}{\tau}=\frac{1}{\tau}\int_{t_{j-1}}^{t_j}(s-t_{j-1})u_{ss}ds.$$

Therefore, we obtain

(48)
$$\begin{aligned}\|\mathbb{W}_1^j\|^2 &= \int_\Omega\left(\frac{1}{\tau}\int_{t_{j-1}}^{t_j}(s-t_{j-1})u_{ss}ds\right)^2dx\\ &\le\frac{1}{\tau^2}\int_\Omega\int_{t_{j-1}}^{t_j}(s-t_{j-1})^2ds\int_{t_{j-1}}^{t_j}u_{ss}^2dsdx\\ &\le C\tau\int_{t_{j-1}}^{t_j}\|u_{ss}\|^2ds.\end{aligned}$$

From the estimate (16), it follows that

$$\sum_{T\in\mathcal{T}_h} h_T\|a(\mathbf{R}_h\nabla u(t_j)-\nabla u(t_j))\|^2_{\partial T}\le Ch^{2k}\|u(t_j)\|^2_{k+1}. \tag{49}$$

Substituting (48) and (49) into (47) yields (38).

To get (39), we take $v=\overline{\partial}e^n$ in (44). It follows that

$$(\overline{\partial}e^n,\overline{\partial}e^n)+a(e^n,\overline{\partial}e^n)=(\mathbb{W}_1^n,\overline{\partial}e^n)-\sum_{T\in\mathcal{T}_h}\langle\mathbb{W}_{2,T}^n,\overline{\partial}e_T^n\rangle_{\partial T},$$

where

$$\begin{aligned}\langle\mathbb{W}_{2,T}^n,\overline{\partial}e_T^n\rangle=&\overline{\partial}\langle\mathbb{W}_{2,T}^n,e_T^n\rangle+\langle(\mathbb{W}_2^n)_t-\overline{\partial}\mathbb{W}_{2,T}^n,e_T^{n-1}\rangle-\langle(\mathbb{W}_2^n)_t,e_T^{n-1}\rangle,\\ (\mathbb{W}_2^n)_t=&a(\nabla u_t(t_n)-\mathbf{R}_h\nabla u_t(t_n))\cdot\mathbf{n}|_T.\end{aligned}$$

Then we arrive at

$$\begin{aligned}&\|\overline{\partial}e^n\|^2+\frac{1}{\tau}a(e^n,e^n)-\frac{1}{\tau}a(e^n,e^{n-1})\\ =&(\mathbb{W}_1^n,\overline{\partial}e^n)-\sum_{T\in\mathcal{T}_h}\Big\{\overline{\partial}\langle\mathbb{W}_{2,T}^n,e_T^n\rangle+\langle(\mathbb{W}_2^n)_t-\overline{\partial}\mathbb{W}_{2,T}^n,e_T^{n-1}\rangle-\langle(\mathbb{W}_2^n)_t,e_T^{n-1}\rangle\Big\},\end{aligned}$$

i.e.

$$\begin{aligned}&\tau\|\overline{\partial}e^n\|^2+a(e^n,e^n)\\ =&a(e^n,e^{n-1})+\tau(\mathbb{W}_1^n,\overline{\partial}e^n)\\ &-\tau\sum_{T\in\mathcal{T}_h}\left\{\overline{\partial}\langle\mathbb{W}_{2,T}^n,e_T^n\rangle+\langle(\mathbb{W}_2^n)_t-\overline{\partial}\mathbb{W}_{2,T}^n,e_T^{n-1}\rangle-\langle(\mathbb{W}_2^n)_t,e_T^{n-1}\rangle\right\}.\end{aligned}$$

Using the Cauchy-Schwarz inequality, the Young inequality, and the trace inequality, we get

(50)

$$\begin{aligned}&\tau\|\overline{\partial}e^n\|^2+a(e^n,e^n)\\ \le&\frac12a(e^n,e^n)+\frac12a(e^{n-1},e^{n-1})+\frac{\tau}{4}\|\mathbb{W}_1^n\|^2+\tau\|\overline{\partial}e^n\|^2\\ &-\tau\left(\sum_{T\in\mathcal{T}_h}\overline{\partial}\left\langle\mathbb{W}_{2,T}^n,e_T^n\right\rangle\right)+\tau\sum_{T\in\mathcal{T}_h}\left(\frac12h_T\|(\mathbb{W}_2^n)_t-\overline{\partial}\mathbb{W}_{2,T}^n\|^2_{\partial T}+\frac12h_T^{-1}\|e_T^{n-1}\|^2_{\partial T}\right)\\ &+\tau\sum_{T\in\mathcal{T}_h}\left(\frac12h_T\|(\mathbb{W}_2^n)_t\|^2_{\partial T}+\frac12h_T^{-1}\|e_T^{n-1}\|^2_{\partial T}\right)\\ \le&\frac12a(e^n,e^n)+\frac12a(e^{n-1},e^{n-1})+\frac{\tau}{4}\|\mathbb{W}_1^n\|^2+\tau\|\overline{\partial}e^n\|^2-\tau\left(\sum_{T\in\mathcal{T}_h}\overline{\partial}\langle\mathbb{W}_{2,T}^n,e_T^n\rangle\right)\\ &+\frac{\tau}{2}\sum_{T\in\mathcal{T}_h}h_T\left(\|(\mathbb{W}_2^n)_t-\overline{\partial}\mathbb{W}_{2,T}^n\|^2_{\partial T}+\|(\mathbb{W}_2^n)_t\|^2_{\partial T}\right)+\tau|\!|\!|e^{n-1}|\!|\!|^2,\end{aligned}$$

where

$$\|\mathbb{W}_{2,T}^j\|^2_{\partial T}=\langle a\left(\nabla u(t_j)-\mathbf{R}_h\nabla u(t_j)\right),a\left(\nabla u(t_j)-\mathbf{R}_h\nabla u(t_j)\right)\rangle_{\partial T}.$$

From the Cauchy-Schwarz inequality and the estimate (23), we obtain

$$\sum_{T\in\mathcal{T}_h}h_T\|\mathbb{W}_{2,T}^j\|^2_{\partial T}$$

$$
\begin{aligned}
&= \sum_{T\in\mathcal{T}_h} h_T \|a\left(\nabla u(t_j) - \mathbf{R}_h \nabla u(t_j)\right)\|_{\partial T}^2 \\
&\le \sum_{T\in\mathcal{T}_h} C\|a\left(\nabla u(t_j) - \mathbf{R}_h \nabla u(t_j)\right)\|_T^2 + h_T^2 \|\nabla\left(a\left(\nabla u(t_j) - \mathbf{R}_h \nabla u(t_j)\right)\right)\|_T^2 \\
&\le C h^{2k}\|u(t_j)\|_{k+1}^2.
\end{aligned}
$$

In a similar way, using the Cauchy-Schwarz inequality and the estimate (23), we have

$$
\sum_{T\in\mathcal{T}_h} h_T\|(\mathbb{W}_2^j)_t - \overline{\partial}\mathbb{W}_2^j\|_{\partial T}^2 \le C\tau \sum_{T\in\mathcal{T}_h} h_T \int_{t_{j-1}}^{t_j} \|(\mathbb{W}_2)_{ss}\|_{\partial T}^2 ds \le C\tau h^{2k}\int_{t_{j-1}}^{t_j}\|u_{ss}\|_{k+1}^2 ds.
$$

Summing (50) from 1 to $n$, we have

$$
\begin{aligned}
\frac{1}{2}a(e^n,e^n) \le& \frac{1}{2}a(e^0,e^0) - \sum_{T\in\mathcal{T}_h}\left(\langle \mathbb{W}_{2,T}^n, e_T^n\rangle - \langle \mathbb{W}_{2,T}^0, e_T^0\rangle\right) \\
&+ \frac{\tau}{4}\sum_{j=1}^n \|\mathbb{W}_1^j\|^2 + \tau\sum_{j=1}^n |\!|\!| e^{j-1}|\!|\!|^2 \\
&+ \tau\sum_{j=1}^n\sum_{T\in\mathcal{T}_h}\left(\frac{h_T}{2}\|(\mathbb{W}_2^j)_t - \overline{\partial}\mathbb{W}_{2,T}^j\|_{\partial T}^2 + \frac{h_T}{2}\|(\mathbb{W}_{2,T}^j)_t\|_{\partial T}^2\right).
\end{aligned}
$$

From (12) and the Cauchy-Schwarz inequality, we have

(51)

$$
\begin{aligned}
\frac{\alpha}{2}|\!|\!| e^n|\!|\!|^2 \le& \frac{\beta}{2}|\!|\!| e^0|\!|\!|^2 + \frac{\tau}{4}\sum_{j=1}^n\|\mathbb{W}_1^j\|^2 + \tau\sum_{j=1}^n|\!|\!| e^{j-1}|\!|\!|^2 \\
&+ \frac{4}{\alpha}\sum_{T\in\mathcal{T}_h} h_T\|\mathbb{W}_{2,T}^n\|_{\partial T}^2 + \frac{\alpha}{4}|\!|\!| e^n|\!|\!|^2 + \frac{1}{2\beta}\sum_{T\in\mathcal{T}_h} h_T\|\mathbb{W}_{2,T}^0\|_{\partial T}^2 + \frac{\beta}{2}|\!|\!| e^0|\!|\!|^2 \\
&+ \tau\sum_{j=1}^n\sum_{T\in\mathcal{T}_h} h_T\|(\mathbb{W}_2^j)_t - \overline{\partial}\mathbb{W}_{2,T}^j\|_{\partial T}^2 + \tau\sum_{j=1}^n\sum_{T\in\mathcal{T}_h} h_T\|(\mathbb{W}_{2,T}^j)_t\|_{\partial T}^2.
\end{aligned}
$$

Combining the above estimates, we arrive at

$$
\begin{aligned}
|\!|\!| e^n|\!|\!|^2 \le& C\Big\{\|e^0\|^2 + |\!|\!| e^0|\!|\!|^2 + h^{2k}\Big(\|u(\cdot,0)\|_{k+1}^2 + \|u\|_{k+1,\infty}^2 \\
&+ \|u_t\|_{k+1,\infty}^2 + \tau^2\int_0^{t_n}\|u_{ss}\|_{k+1}^2 ds\Big) + \tau^2\int_0^{t_n}\|u_{ss}\|^2 ds\Big\}.
\end{aligned}
$$

This completes the proof of the theorem. □

## 4. Optimal order error estimate

Theorem 2.2 and Theorem 3.3 show that the $L^2$ errors of both the semi-discrete and full-discrete schemes have not reached the optimal order. To derive optimal order error estimate, the elliptic projection method is used for analysis.

**Definition 4.1.** *For any $u\in H_0^1(\Omega)$, we define the elliptic projection $\mathcal{E}_h : H_0^1(\Omega)\to V_h$ satisfying*

(52) $$a(\mathcal{E}_h u,\chi) = (-\nabla\cdot(a\nabla u),\chi), \quad \forall\,\chi\in V_h.$$

Then $\mathcal{E}_h u$ can be seen as a CDG numerical solution of the elliptic problem:

(53) $$\begin{cases} -\nabla\cdot(a\nabla u) &= f, \quad \text{in } \Omega, \\ u &= 0, \quad \text{on } \partial\Omega. \end{cases}$$

Regarding elliptical projection $\mathcal{E}_h$, the following error estimates are presented [26].

**Lemma 4.1.** *[26] Let $u \in H^{k+1}(\Omega)$, there holds*

$$\|\!|\mathcal{E}_h u - u\|\!| \le Ch^k \|u\|_{k+1}, \tag{54}$$

$$\|\mathcal{E}_h u - u\| \le Ch^{k+1} \|u\|_{k+1}. \tag{55}$$

**4.1. Optimal order error estimate for the semi-discrete CDG scheme.** This section mainly derives the error estimate of optimal order in $L^2$-norm for the semi-discrete CDG scheme (7). This section also provides the $H^1$ error estimate based on elliptic projection for the article's completeness.

**Theorem 4.1.** *Let $u \in C^1\left(0, \overline{T}; H^{k+1}(\Omega)\right)$ be exact solution of the (1) and $u_h(t) \in C^1\left(0, \overline{T}; V_h^0\right)$ be the numerical solution of the semi-discrete CDG scheme (7), there holds*

$$\|u_h(t) - u(t)\| \le \|u_h(0) - u(0)\| + Ch^{k+1}\left(\|\psi\|_{k+1} + \int_0^t \|u_s\|_{k+1} ds\right). \tag{56}$$

*Proof.* Let $\zeta = u_h - \mathcal{E}_h u$ and $\vartheta = \mathcal{E}_h u - u$, then

$$u_h(t) - u(t) = \zeta(t) + \vartheta(t). \tag{57}$$

From Lemma 4.1, we have

$$\|\vartheta\| \le Ch^{k+1}\|u\|_{k+1} \le Ch^{k+1}\left(\|\psi\|_{k+1} + \int_0^t \|u_s\|_{k+1} ds\right). \tag{58}$$

According to the definition of the $\mathcal{E}_h$, we get

$$\begin{aligned}
(\zeta_t, \chi) + a(\zeta, \chi) &= ((u_h)_t, \chi) - (\mathcal{E}_h u_t, \chi) + a\left(u_h, \chi\right) - a\left(\mathcal{E}_h u, \chi\right) \\
&= (f, \chi) - (\mathcal{E}_h u_t, \chi) - a(\mathcal{E}_h u, \chi) \\
&= (f, \chi) - (\mathcal{E}_h u_t, \chi) + (\nabla \cdot (a \nabla u), \chi) \\
&= (u_t, \chi) - (\mathcal{E}_h u_t, \chi) \\
&= -(\vartheta_t, \chi).
\end{aligned} \tag{59}$$

Since $\zeta \in V_h$ and $\chi \in V_h$, we take $\chi = \zeta$ in (59) and obtain

$$(\zeta_t, \zeta) + a(\zeta, \zeta) = -(\vartheta_t, \zeta), \quad t > 0.$$

From the coercive of the bilinear form $a(\cdot, \cdot)$ as (12), we get

$$(\zeta_t, \zeta) = \frac{1}{2}\frac{d}{dt}\|\zeta\|^2 = \|\zeta\|\frac{d}{dt}\|\zeta\| \le \|\vartheta_t\|\|\zeta\|,$$

which yields

$$\frac{d}{dt}\|\zeta\| \le \|\vartheta_t\|.$$

Integrating the above equation with respect to $t$, we arrive at

$$\int_0^t \frac{d}{dt}\|\zeta\| ds \le \int_0^t \|\vartheta_s\| ds,$$

which leads to

$$\|\zeta(t)\| \le \|\zeta(0)\| + \int_0^t \|\vartheta_s\| ds. \tag{60}$$

According to Lemma 4.1, we get

$$\begin{aligned}
\|\zeta(0)\| &= \|u_h(0) - \mathcal{E}_h u(0)\| \\
&\le \|u_h(0) - u(0)\| + \|\mathcal{E}_h u(0) - u(0)\| \\
&\le \|u_h(0) - u(0)\| + Ch^{k+1}\|\psi\|_{k+1},
\end{aligned} \tag{61}$$

and

$$\|\vartheta_t\| \le Ch^{k+1}\|u_t\|_{k+1}. \tag{62}$$

Combining above estimates yields

$$\begin{aligned}\|u_h(t)-u(t)\| &= \|\zeta(t)+\vartheta(t)\| \\ &\le \|\zeta(t)\|+\|\vartheta(t)\| \\ &\le \|u_h(0)-u(0)\| + Ch^{k+1}\left(\|\psi\|_{k+1}+\int_0^t \|u_s\|_{k+1}ds\right).\end{aligned}$$

This completes the proof. □

**Theorem 4.2.** *Assume that $u \in C^1\left(0,\overline{T};H^{k+1}(\Omega)\right)$ is exact solution of the (1) and $u_h(t) \in C^1\left(0,\overline{T};V_h^0\right)$ is the numerical solution of the semi-discrete CDG scheme (7), we have*

$$\begin{aligned}&|\!|\!|u_h(t)-u(t)|\!|\!|^2 \\ \le& \frac{2\beta}{\alpha}|\!|\!|u_h(0)-u(0)|\!|\!|^2 + Ch^{2k}\left(\|\psi\|_{k+1}^2+\|u\|_{k+1}^2\right)+Ch^{2(k+1)}\int_0^t \|u_s\|_{k+1}^2 ds.\end{aligned} \tag{63}$$

*Proof.* From Lemma 4.1, we have

$$|\!|\!|\vartheta(t)|\!|\!| = |\!|\!|\mathcal{E}_h u(t)-u(t)|\!|\!| \le Ch^k\|u\|_{k+1}. \tag{64}$$

Letting $\chi=\zeta_t$ in (59) yields

$$(\zeta_t,\zeta_t)+a(\zeta,\zeta_t) = -(\vartheta_t,\zeta_t). \tag{65}$$

Using the Young inequality, we get

$$\|\zeta_t\|^2+\frac{1}{2}\frac{d}{dt}a(\zeta,\zeta) = -(\vartheta_t,\zeta_t) \le \frac{1}{2}\|\vartheta_t\|^2+\frac{1}{2}\|\zeta_t\|^2, \tag{66}$$

which leads to

$$\frac{d}{dt}a(\zeta,\zeta) \le \|\vartheta_t\|^2.$$

Integrating the above equation with respect to $t$, we arrive at

$$a(\zeta,\zeta) \le a\left(\zeta(0),\zeta(0)\right) + \int_0^t \|\vartheta_s\|^2 ds, \tag{67}$$

where

$$a\left(\zeta(0),\zeta(0)\right) = \sum_{T\in\mathcal{T}_h}\Big(a\nabla_w(u_h(0)-\mathcal{E}_h u(0)),\nabla_w(u_h(0)-\mathcal{E}_h u(0))\Big)_T. \tag{68}$$

From Lemma 4.1, it follows that

$$\begin{aligned}\alpha|\!|\!|\zeta|\!|\!|^2 \le& a(\zeta(0),\zeta(0))+\int_0^t \|\vartheta_s\|^2 ds \\ \le& 2a\left(u_h(0)-u(0),u_h(0)-u(0)\right) \\ &+2a\left(\mathcal{E}_h u(0)-u(0),\mathcal{E}_h u(0)-u(0)\right)+\int_0^t \|\vartheta_s\|^2 ds \\ \le& 2\beta\left(|\!|\!|u_h(0)-u(0)|\!|\!|^2+|\!|\!|\mathcal{E}_h u(0)-u(0)|\!|\!|^2\right)+\int_0^t \|\vartheta_s\|^2 ds \\ \le& 2\beta|\!|\!|u_h(0)-u(0)|\!|\!|^2 + Ch^{2k}\|\psi\|_{k+1}^2 + Ch^{2(k+1)}\int_0^t \|u_s\|_{k+1}^2 ds.\end{aligned} \tag{69}$$

Combining the above estimates gives

$$\begin{aligned}\|u_h(t)-u(t)\|^2 \leq & \frac{2\beta}{\alpha}\|u_h(0)-u(0)\|^2 + Ch^{2k}\left(\|\psi\|_{k+1}^2 + \|u\|_{k+1}^2\right) \\ & + Ch^{2(k+1)}\int_0^t \|u_s\|_{k+1}^2 ds.\end{aligned}$$

The proof is completed. □

**4.2. Optimal order error estimate for the full-discrete CDG scheme.** This section primarily establishes the optimal convergence order in $L^2$-norm concerning the full-discrete CDG scheme (30). Moreover, it offers an analysis of the $H^1$ error estimate employing elliptic projection, thus contributing to the overall comprehensiveness and rigor of the research article.

**Theorem 4.3.** *Let $u \in C^2\left(0,\overline{T};\ H^{k+1}(\Omega)\right)$ be the exact solution of the parabolic equation (1), $U^n$ be the CDG solution of the full-discrete CDG scheme (30). There exists a constant $C>0$, such that*

$$\begin{aligned}&\|U^n - u(t_n)\| \\ &\leq \|U^0 - u(0)\| + Ch^{k+1}\left(\|\psi\|_{k+1} + \int_0^{t_n}\|u_s\|_{k+1}ds\right) + C\tau\int_0^{t_n}\|u_{ss}\|ds.\end{aligned} \tag{70}$$

*Proof.* Let

$$U^n - u(t_n) = (U^n - \mathcal{E}_h u(t_n)) + (\mathcal{E}_h u(t_n) - u(t_n)) = \zeta^n + \vartheta^n. \tag{71}$$

From Lemma 4.1, we have

$$\|\vartheta^n\| = \|\mathcal{E}_h u(t_n) - u(t_n)\| \leq Ch^{k+1}\left(\|\psi\|_{k+1} + \int_0^{t_n}\|u_s\|_{k+1}ds\right). \tag{72}$$

According to the definition of the $\mathcal{E}_h$, it follows that

$$\begin{aligned}(\overline{\partial}\zeta^n,\chi) + a(\zeta^n,\chi) &= \left(\overline{\partial}U^n,\chi\right) - \left(\overline{\partial}\mathcal{E}_h u(t_n),\chi\right) + a\left(U^n,\chi\right) - a\left(\mathcal{E}_h u(t_n),\chi\right) \\ &= (f(t_n),\chi) - \left(\overline{\partial}\mathcal{E}_h u(t_n),\chi\right) - a\left(\mathcal{E}_h u(t_n),\chi\right) \\ &= (f(t_n),\chi) - \left(\overline{\partial}\mathcal{E}_h u(t_n),\chi\right) + (\nabla\cdot(a\nabla u(t_n))) \\ &= (u_t(t_n),\chi) - \left(\overline{\partial}\mathcal{E}_h u(t_n),\chi\right) \\ &= \left(u_t(t_n) - \overline{\partial}u(t_n),\chi\right) + \left(\overline{\partial}u(t_n) - \overline{\partial}\mathcal{E}_h u(t_n),\chi\right),\end{aligned} \tag{73}$$

which leads to

$$\left(\overline{\partial}\zeta^n,\chi\right) + a\left(\zeta^n,\chi\right) = \left(\mathbb{W}_1^n,\chi\right) + \left(\mathbb{W}_3^n,\chi\right) = \left(\mathbb{W}^n,\chi\right), \tag{74}$$

with

$$\begin{aligned}\mathbb{W}_1^n &= u_t(t_n) - \overline{\partial}u(t_n), \\ \mathbb{W}_3^n &= \overline{\partial}u(t_n) - \overline{\partial}\mathcal{E}_h u(t_n).\end{aligned}$$

Taking $\chi = \zeta^n$ in (74), we obtain

$$\left(\overline{\partial}\zeta^n,\zeta^n\right) + a(\zeta^n,\zeta^n) = (\mathbb{W}^n,\zeta^n), \tag{75}$$

which yields

$$\left(\overline{\partial}\zeta^n,\zeta^n\right) \leq \|\mathbb{W}^n\|\cdot\|\zeta^n\|.$$

Then we get

$$\frac{1}{\tau}\left(\|\zeta^n\|^2 - (\zeta^{n-1},\zeta^n)\right) \leq \|\mathbb{W}^n\|\cdot\|\zeta^n\|,$$

which implies that

$$\|\zeta^n\| \le \tau\|\mathbb{W}^n\| + \|\zeta^{n-1}\|.$$

Using induction, it is simple to get that

$$\|\zeta^n\| \le \tau\sum_{j=1}^{n}\|\mathbb{W}^j\| + \|\zeta^0\| \le \tau\sum_{j=1}^{n}\|\mathbb{W}_1^j\| + \tau\sum_{j=1}^{n}\|\mathbb{W}_3^j\| + \|\zeta^0\|. \tag{76}$$

According to Theorem 3.3, we get

$$\tau\sum_{j=1}^{n}\|\mathbb{W}_1^j\| \le \tau\int_0^{t_n}\|u_{ss}\|ds. \tag{77}$$

Note that

$$\mathbb{W}_3^j = \frac{1}{\tau}\left(I-\mathcal{E}_h\right)\int_{t_{j-1}}^{t_j} u_s ds = \frac{1}{\tau}\int_{t_{j-1}}^{t_j}\left(I-\mathcal{E}_h\right)u_s ds,$$

then we obtain

$$\tau\sum_{j=1}^{n}\|\mathbb{W}_3^j\| \le Ch^{k+1}\int_0^{t_n}\|u_s\|_{k+1}ds. \tag{78}$$

Combining above estimates, we arrive at

$$\begin{aligned}\|U^n - u(t_n)\| \le& \|\zeta^n\| + \|\vartheta^n\| \\ \le& \|\zeta^0\| + \tau\int_0^{t_n}\|u_{ss}\|ds + Ch^{k+1}\int_0^{t_n}\|u_s\|_{k+1}ds \\ &+ Ch^{k+1}\left(\|\psi\|_{k+1} + \int_0^{t_n}\|u_s\|_{k+1}ds\right) \\ \le& \|U^0 - u(0)\| + Ch^{k+1}\left(\|\psi\|_{k+1} + \int_0^{t_n}\|u_s\|_{k+1}ds\right) \\ &+ C\tau\int_0^{t_n}\|u_{ss}\|ds.\end{aligned}$$

The proof is completed. □

**Theorem 4.4.** *Let $u \in C^2\left(0,\overline{T};H^{k+1}(\Omega)\right)$ be the exact solution of the parabolic equation (1), $U^n$ be the CDG solution of the full-discrete CDG scheme (30). There exists a constant $C>0$, such that*

$$\begin{aligned}|\!|\!|U^n - u(t_n)|\!|\!|^2 \le& 2|\!|\!|U^0 - u(0)|\!|\!|^2 + C\Big\{h^{2k}\left(\|\psi\|_{k+1}^2 + \int_0^{t_n}\|u\|_{k+1}^2ds\right) \\ &+ h^{2(k+1)}\int_0^{t_n}\|u\|_{k+1}^2ds + \tau^2\int_0^{t_n}\|u_{ss}\|^2ds\Big\}.\end{aligned} \tag{79}$$

*Proof.* According to Theorem 4.3, we have $U^n - u(t_n) = \zeta^n + \vartheta^n$. From Lemma 4.1, it follows that

$$|\!|\!|\vartheta^n|\!|\!|^2 \le Ch^{2k}\|u\|_{k+1}^2. \tag{80}$$

By taking $\chi = \overline{\partial}\zeta^n$ in (74), we obtain

$$\|\overline{\partial}\zeta^n\|^2 + \frac{\tau}{2}a\left(\overline{\partial}\zeta^n,\overline{\partial}\zeta^n\right) + \frac{1}{2}\overline{\partial}a(\zeta^n,\zeta^n) = \left(\mathbb{W}^n,\overline{\partial}\zeta^n\right) \le \frac{1}{2}\|\mathbb{W}^n\|^2 + \frac{1}{2}\|\overline{\partial}\zeta^n\|^2. \tag{81}$$

Using the coercive of the bilinear form $a(\cdot,\cdot)$ as (12), we get

$$\alpha\overline{\partial}|\!|\!|\zeta^n|\!|\!|^2 \le \|\mathbb{W}^n\|^2, \tag{82}$$

then we obtain

$$\|\!|\zeta^n\|\!|^2 \le \frac{\tau}{\alpha}\|\mathbb{W}^n\|^2 + \|\!|\zeta^{n-1}\|\!|^2. \tag{83}$$

By induction, then we get

$$\|\!|\zeta^n\|\!|^2 \le \frac{\tau}{\alpha}\sum_{j=1}^{n}\|\mathbb{W}^j\|^2 + \|\!|\zeta^0\|\!|^2 \le \frac{2\tau}{\alpha}\sum_{j=1}^{n}\|\mathbb{W}_1^j\|^2 + \frac{2\tau}{\alpha}\sum_{j=1}^{n}\|\mathbb{W}_3^j\|^2 + \|\!|\zeta^0\|\!|^2. \tag{84}$$

Similar to (77) and (78), it is easy to get that

$$\tau\sum_{j=1}^{n}\|\mathbb{W}_1^j\|^2 \le \tau^2\int_0^{t_n}\|u_{ss}\|^2 ds, \tag{85}$$

and

$$\begin{aligned}
\tau\sum_{j=1}^{n}\|\mathbb{W}_3^j\|^2 &= \tau\sum_{j=1}^{n}\int_\Omega\left(\frac{1}{\tau}\int_{t_{j-1}}^{t_j}\vartheta_s ds\right)^2 dx\\
&\le \sum_{j=1}^{n}\int_\Omega\int_{t_{j-1}}^{t_j}\vartheta_s^2 ds dx\\
&\le \sum_{j=1}^{n}\int_{t_{j-1}}^{t_j}\|\vartheta_s\|^2 ds\\
&\le \int_0^{t_n}\|\vartheta_s\|^2 ds\\
&\le Ch^{2(k+1)}\int_0^{t_n}\|u\|_{k+1}^2 ds.
\end{aligned} \tag{86}$$

According to Lemma 4.1, we obtain

$$\|\!|\zeta^0\|\!|^2 \le 2\left(\|\!|U^0 - u(0)\|\!|^2 + Ch^{2k}\|\psi\|_{k+1}^2\right),$$

Combining above yields

$$\begin{aligned}
\|\!|U^n - u(t_n)\|\!|^2 \le 2\|\!|U^0 - u(0)\|\!|^2 + C\Big\{h^{2k}\left(\|\psi\|_{k+1}^2 + \int_0^{t_n}\|u\|_{k+1}^2 ds\right)\\
+ h^{2(k+1)}\int_0^{t_n}\|u\|_{k+1}^2 ds + \tau^2\int_0^{t_n}\|u_{ss}\|^2 ds\Big\}.
\end{aligned}$$

This completes the proof of the Theorem. □

**Remark 4.1.** *According to Theorem 4.3 and Theorem 4.4, the errors are* $O(\tau + h^k)$ *in the* $H^1$ *norm and* $O(\tau + h^{k+1})$ *in the* $L^2$ *norm with* $P_k$ *CDG elements, respectively.*

**Remark 4.2.** *(a) For simplicity, we only considered the results for the two - dimensional case. This result can be readily extended to three-dimensional situations.*
*(b) In this paper, we use the CDG method to solve the second-order parabolic equation with homogeneous Dirichlet boundary conditions. What's more, the CDG approach used in this manuscript can be readily generalized to nonhomogeneous Dirichlet and mixed Dirichlet-Neumann boundary conditions. Nonhomogeneous Dirichlet boundary conditions require modification solely in the approximation function space.*

*Mixed Dirichlet-Neumann boundary conditions require adjustments to both the approximation function space and the right-hand side of the numerical scheme. The analysis of well-posedness and error estimates follows a similar way.*

## 5. Numerical experiments

In this section, we give some numerical experiments to validate the effectiveness of the CDG scheme.

**Example 5.1.** *(Constant Coefficients) Consider the parabolic equation (1) in a square domain $\Omega = (0,1)\times(0,1)$. The exact solution is choose as follows*

$$u = e^{-t}\sin(\pi x)\sin(\pi y).$$

*where the coefficient matrix* $a = \begin{pmatrix}1 & 0\\ 0 & 1\end{pmatrix}$, *and the final time* $\overline{T} = 1$.

In this example, we use triangular meshes. The numerical results of Example 5.1 are shown in Tables 1-3. As evidenced by the results presented in Tables 1-3, it is apparent that the numerical results attained the optimal convergence order on triangular meshes, which is compatible with the theoretical analysis.

TABLE 1. Numerical results by the $P_1$ CDG element with $\tau = 2h^2$ on triangular meshes in Example 5.1.

| 1/h | $\|\|\|u-u_h\|\|\|$ | order | $\|u-u_h\|$ | order |
|---|---|---|---|---|
| 4 | 8.2193E-01 | – | 2.2944E-02 | – |
| 8 | 2.9045E-01 | 1.5007 | 4.1023E-03 | 2.4836 |
| 16 | 1.1455E-01 | 1.3423 | 8.1499E-04 | 2.3316 |
| 32 | 4.9838E-02 | 1.2007 | 1.7803E-04 | 2.1946 |
| 64 | 2.3151E-02 | 1.1062 | 4.1438E-05 | 2.1031 |

TABLE 2. Numerical results by the $P_2$ CDG element with $\tau = (\sqrt{2}h)^3$ on triangular meshes in Example 5.1.

| 1/h | $\|\|\|u-u_h\|\|\|$ | order | $\|u-u_h\|$ | order |
|---|---|---|---|---|
| 4 | 1.4282E-01 | – | 2.9235E-03 | – |
| 8 | 3.8847E-02 | 1.8784 | 3.8294E-04 | 2.9325 |
| 16 | 7.2408E-03 | 2.4236 | 3.5685E-05 | 3.4237 |
| 32 | 1.5490E-03 | 2.2249 | 3.8027E-06 | 3.2302 |

TABLE 3. Numerical results by the $P_3$ CDG element with $\tau = (\frac{1}{512})^2$ on triangular meshes in Example 5.1.

| 1/h | $\|\|\|u-u_h\|\|\|$ | order | $\|u-u_h\|$ | order |
|---|---|---|---|---|
| 2 | 1.2087E-01 | – | 3.5326E-03 | – |
| 4 | 1.2313E-02 | 3.2952 | 1.8198E-04 | 4.2789 |
| 8 | 1.2767E-03 | 3.2697 | 9.5109E-06 | 4.2580 |
| 16 | 1.5209E-04 | 3.0693 | 5.4159E-07 | 4.1343 |

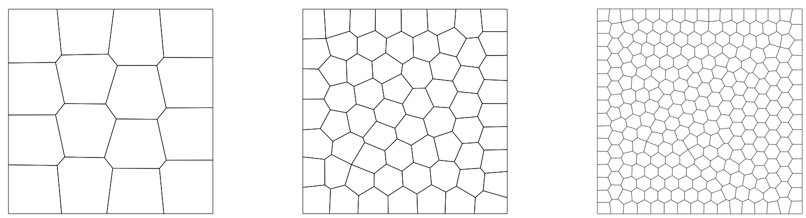

FIGURE 1. The polygonal meshes with $h = \frac{1}{4}, \frac{1}{8}, \frac{1}{16}$.

**Example 5.2.** *(Constant Coefficient) In this example, we consider the same problem as Example 5.1. This example focus shifts towards investigating the convergence order with respect to time step $\tau$. In this example, computations are conducted using triangular, rectangular, and polygonal meshes. The polygonal meshes are shown in Figure 1.*

We fix the mesh size $h = 1/32$ and obtain the convergence order with respect to time step $\tau$. Tables 4-6 present the errors and the convergence orders about $H^1$ and $L^2$ norms with respect to temporal discretization, showing a convergence rate of $O(\tau)$, thus verifying the consistency with theoretical analysis.

TABLE 4. Numerical results by the $P_2$ CDG element with $h = 1/32$ on triangular meshes in Example 5.2.

| $1/\tau$ | $\|\|\|u - u_h\|\|\|$ | order | $\|u - u_h\|$ | order |
|---|---|---|---|---|
| 4 | 6.4027E-01 | – | 1.3368E-03 | – |
| 8 | 3.0465E-01 | 1.0715 | 6.3606E-04 | 1.0715 |
| 16 | 1.4744E-01 | 1.0470 | 3.0785E-04 | 1.0470 |
| 32 | 7.1467E-02 | 1.0448 | 1.4923E-04 | 1.0447 |
| 64 | 3.4139E-02 | 1.0658 | 7.1290E-05 | 1.0657 |
| 128 | 1.5681E-02 | 1.1224 | 3.2743E-05 | 1.1225 |

TABLE 5. Numerical results by the $P_2$ CDG element with $h = 1/32$ on rectangular meshes in Example 5.2.

| $1/\tau$ | $\|\|\|u - u_h\|\|\|$ | order | $\|u - u_h\|$ | order |
|---|---|---|---|---|
| 4 | 5.5196E-01 | – | 1.3313E-03 | – |
| 8 | 2.6149E-01 | 1.0778 | 6.3067E-04 | 1.0779 |
| 16 | 1.2544E-01 | 1.0597 | 3.0250E-04 | 1.0600 |
| 32 | 5.9711E-02 | 1.0710 | 1.4395E-04 | 1.0714 |
| 64 | 2.7454E-02 | 1.1210 | 6.6157E-05 | 1.1216 |
| 128 | 1.1613E-02 | 1.2413 | 2.7982E-05 | 1.2414 |

**Example 5.3.** *(Variable Coefficient) Consider the parabolic equation (1) in a square domain $\Omega = (0,1) \times (0,1)$ with the final time $\overline{T} = 1$. The exact solution is given by*

$$u = e^{-t} \sin(\pi x) \cos(\pi y),$$

TABLE 6. Numerical results by the $P_2$ CDG element with $h = 1/32$ on polygonal meshes in Example 5.2.

| $1/\tau$ | $\|\|\|u - u_h\|\|\|$ | order | $\|\|u - u_h\|\|$ | order |
|---|---|---|---|---|
| 4 | 6.5313E-01 | – | 1.3348E-03 | – |
| 8 | 3.1029E-01 | 1.0738 | 6.3415E-04 | 1.0738 |
| 16 | 1.4970E-01 | 1.0515 | 3.0595E-04 | 1.0515 |
| 32 | 7.2104E-02 | 1.0540 | 1.4736E-04 | 1.0540 |
| 64 | 3.3989E-02 | 1.0850 | 6.9466E-05 | 1.0849 |
| 128 | 1.5173E-02 | 1.1636 | 3.1032E-05 | 1.1625 |

*where the coefficient matrix*

$$a = \begin{pmatrix} x^2 + y^2 + 1 & xy \\ xy & x^2 + y^2 + 1 \end{pmatrix}.$$

*In this example, we use rectangular meshes and polygonal meshes.*

The errors and corresponding convergence orders are listed in Tables 7-10. From Tables 7-10, it can be seen that within rectangular or polygonal meshes and under the $H^1$-norm, the convergence order manifests as $O(h^1)$ when employing the $P_1$ CDG element and as $O(h^2)$ when using the $P_2$ CDG element. Under the $L^2$-norm, Tables 7-10 indicate that the $P_1$ CDG element achieves the convergence order of $O(h^2)$, while the $P_2$ CDG element exhibits the convergence order of $O(h^3)$. This is consistent with the previous theoretical analysis results.

TABLE 7. Numerical results by the $P_1$ CDG element with $\tau = h$ on rectangular meshes in Example 5.3.

| 1/h | $\|\|\|u - u_h\|\|\|$ | order | $\|\|u - u_h\|\|$ | order |
|---|---|---|---|---|
| 4 | 2.1814E+00 | – | 3.9742E-02 | – |
| 8 | 8.4981E-01 | 1.3601 | 8.2486E-03 | 2.2684 |
| 16 | 3.8689E-01 | 1.1352 | 1.9423E-03 | 2.0864 |
| 32 | 1.8797E-01 | 1.0414 | 4.7756E-04 | 2.0240 |
| 64 | 9.3188E-02 | 1.0123 | 1.1864E-04 | 2.0091 |

TABLE 8. Numerical results by the $P_2$ CDG element with $\tau = h^2$ on rectangular meshes in Example 5.3.

| 1/h | $\|\|\|u - u_h\|\|\|$ | order | $\|\|u - u_h\|\|$ | order |
|---|---|---|---|---|
| 4 | 2.3221E-01 | – | 2.8743E-03 | – |
| 8 | 6.0912E-02 | 1.9306 | 4.0236E-04 | 2.8366 |
| 16 | 1.5031E-02 | 2.0188 | 5.0694E-05 | 2.9886 |
| 32 | 3.7012E-03 | 2.0219 | 6.2652E-06 | 3.0164 |
| 64 | 9.1333E-04 | 2.0188 | 7.7411E-07 | 3.0168 |

**Example 5.4.** *(L-Shaped Domain) Consider the parabolic equation (1) in the L-shaped domain* $\Omega = (0,1)^2 \setminus (0.5,1) \times (0,0.5)$ *with the final time* $\overline{T} = 1$*. The exact solution is*

$$u = e^{-t} \sin(\pi x) \sin(\pi y),$$

TABLE 9. Numerical results by the $P_1$ CDG element with $\tau = h$ on polygonal meshes in Example 5.3.

| 1/h | $\|\|\|u - u_h\|\|\|$ | order | $\|\|u - u_h\|\|$ | order |
|---|---|---|---|---|
| 4 | 1.8855E+00 | – | 2.2140E-02 | – |
| 8 | 1.1208E+00 | 0.7504 | 8.1353E-03 | 1.4444 |
| 16 | 5.7714E-01 | 0.9575 | 2.3167E-03 | 1.8122 |
| 32 | 2.8597E-01 | 1.0131 | 6.0110E-04 | 1.9464 |
| 64 | 1.3990E-01 | 1.0314 | 1.5026E-04 | 2.0001 |

TABLE 10. Numerical results by the $P_2$ CDG element with $\tau = h^2$ on polygonal meshes in Example 5.3.

| 1/h | $\|\|\|u - u_h\|\|\|$ | order | $\|\|u - u_h\|\|$ | order |
|---|---|---|---|---|
| 2 | 5.5330E-01 | – | 9.6754E-03 | – |
| 4 | 1.5312E-01 | 1.8537 | 1.5492E-03 | 2.6427 |
| 8 | 3.8764E-02 | 1.9794 | 1.9462E-04 | 2.9907 |
| 16 | 8.4499E-03 | 2.1990 | 2.0800E-05 | 3.2288 |
| 32 | 1.9146E-03 | 2.1454 | 2.4092E-06 | 3.1095 |

*where the coefficient matrix* $a = \begin{pmatrix} 2 & 1 \\ 1 & 3 \end{pmatrix}$.

In this example, we use triangular meshes shown in Figure 2. Tables 11-12 present errors and convergence rates. The results indicate that the CDG scheme with $P_k$ elements obtains convergence rates of $O(h^{k+1})$ and $O(h^k)$ in the $L^2$ and $H^1$ norms, respectively. These results align with theoretical analyses.

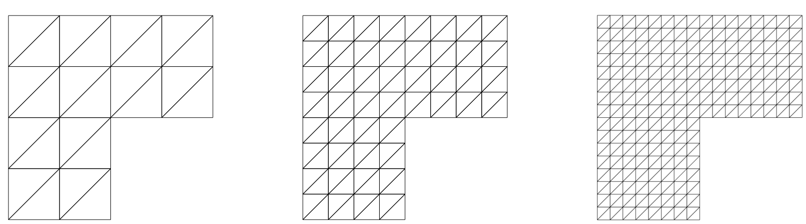

FIGURE 2. The triangular meshes on L-shaped domain with $h = \frac{1}{4}, \frac{1}{8}, \frac{1}{16}$.

TABLE 11. Numerical results by the $P_1$ CDG element with $\tau = h/2$ on triangular meshes in Example 5.4.

| $1/\tau$ | $\|\|\|u - u_h\|\|\|$ | order | $\|\|u - u_h\|\|$ | order |
|---|---|---|---|---|
| 4 | 1.9614E+00 | – | 2.6564E-02 | – |
| 8 | 1.2062E+00 | 0.7014 | 8.3570E-03 | 1.6684 |
| 16 | 6.4091E-01 | 0.9123 | 2.2393E-03 | 1.9000 |
| 32 | 3.2651E-01 | 0.9730 | 5.7191E-04 | 1.9692 |
| 64 | 1.6449E-01 | 0.9892 | 1.4417E-04 | 1.9880 |

TABLE 12. Numerical results by the $P_2$ CDG element with $\tau = h^2$ on triangular meshes in Example 5.4.

| $1/\tau$ | $\|\|\|u-u_h\|\|\|$ | order | $\|\|u-u_h\|\|$ | order |
|---|---|---|---|---|
| 2 | 8.5413E-02 | – | 1.3811E-03 | – |
| 4 | 2.0892E-02 | 2.0307 | 1.9529E-04 | 2.8231 |
| 8 | 5.0655E-03 | 2.0434 | 2.5626E-05 | 2.9293 |
| 16 | 1.2906E-03 | 1.9746 | 3.3506E-06 | 2.9339 |
| 32 | 3.3632E-04 | 1.9408 | 4.4002E-07 | 2.9286 |

**Example 5.5.** *(Low regularity) Consider the parabolic equation (1) in a square domain $\Omega = (0,1)\times(0,1)$ with the final time $\overline{T} = 1$ and the coefficient matrix*

$$a = \begin{pmatrix} x^2+y^2+1 & xy \\ xy & x^2+y^2+1 \end{pmatrix}.$$

*Choose initial values $\psi$ and source terms $f$ such that the exact solution is [8]*

$$u = e^{-t}x(1-x)y(1-y)\left(\sqrt{x^2+y^2}\right)^{-2+\gamma}, \quad 0<\gamma\le 1.$$

*For any $0<\varepsilon<\gamma$, let $\delta = \gamma-\varepsilon > 0$. It is known from [8] that the exact solution has low regularity, i.e. $u(\cdot,t)\in H^{1+\delta}(\Omega)\cap H_1^0(\Omega)$, $0<\delta<1$,and $u(\cdot,t)\notin H^{1+\gamma}(\Omega)$.*

We provide the error and spatial convergence order for $\gamma = 0.25$ and $\gamma = 0.75$ in Tables 13-15. Tables 13-15 show that for $\gamma = 0.25$, the spatial convergence order is 1.25, and for $\gamma = 0.75$, it is 1.75, consistent with the regularity of the exact solution.

TABLE 13. Numerical results by the $P_1$ CDG element with $\tau = h$ on triangular meshes in Example 5.5.

| 1/h | $\gamma = 0.25$ | | $\gamma = 0.75$ | |
|---|---|---|---|---|
| | $\|\|u-u_h\|\|$ | order | $\|\|u-u_h\|\|$ | order |
| 4 | 4.3737E-02 | – | 1.0192E-02 | – |
| 8 | 1.9430E-02 | 1.1706 | 3.2865E-03 | 1.6328 |
| 16 | 8.2544E-03 | 1.2350 | 9.7724E-04 | 1.7498 |
| 32 | 3.4587E-03 | 1.2549 | 2.8133E-04 | 1.7964 |
| 64 | 1.4457E-03 | 1.2585 | 8.0469E-05 | 1.8058 |

TABLE 14. Numerical results by the $P_1$ CDG element with $\tau = h$ on rectangular meshes in Example 5.5.

| 1/h | $\gamma = 0.25$ | | $\gamma = 0.75$ | |
|---|---|---|---|---|
| | $\|\|u-u_h\|\|$ | order | $\|\|u-u_h\|\|$ | order |
| 4 | 5.3701E-02 | – | 1.2453E-02 | – |
| 8 | 2.3526E-02 | 1.1907 | 3.8357E-03 | 1.6990 |
| 16 | 9.8953E-03 | 1.2494 | 1.0869E-03 | 1.8193 |
| 32 | 4.1358E-03 | 1.2586 | 3.0855E-04 | 1.8166 |
| 64 | 1.7292E-03 | 1.2580 | 8.9445E-05 | 1.7864 |

TABLE 15. Numerical results by the $P_1$ CDG element with $\tau = h$ on polygonal meshes in Example 5.5.

| 1/h | $\gamma = 0.25$ | | $\gamma = 0.75$ | |
|---|---|---|---|---|
| | $\|u - u_h\|$ | order | $\|u - u_h\|$ | order |
| 4 | 2.7957E-02 | – | 3.8524E-03 | – |
| 8 | 1.1619E-02 | 1.2667 | 1.1134E-03 | 1.7907 |
| 16 | 4.8574E-03 | 1.2582 | 3.2496E-04 | 1.7767 |
| 32 | 2.0380E-03 | 1.2530 | 9.5927E-05 | 1.7603 |
| 64 | 8.5577E-04 | 1.2519 | 2.8718E-05 | 1.7409 |

In the following example, we consider the the second-order parabolic equation with a mixed Dirichlet-Neumann boundary condition: Find $u$ satisfies

$$
\begin{cases} u_t - \nabla\cdot(a\nabla u) &= f, \quad \mathbf{x}\in\Omega,\ t\in J,\\ u(\cdot,0) &= \psi, \quad \mathbf{x}\in\Omega,\\ u &= \widehat{g}, \quad \mathbf{x}\in\Gamma_D,\ t\in J,\\ (a\nabla u)\cdot\mathbf{n} &= \widehat{t}, \quad \mathbf{x}\in\Gamma_N,\ t\in J, \end{cases} \tag{87}
$$

where $\Gamma_D \cup \Gamma_N = \partial\Omega$, $\Gamma_D \cap \Gamma_N = \emptyset$, and $|\Gamma_D| > 0$.

**Example 5.6.** *(Mixed Dirichlet-Neumann boundary condition) Consider problem (87) in a square domain $\Omega = (0,1)^2$ with the final time $\overline{T} = 1$ and the coefficient matrix*

$$
a = \begin{pmatrix} x^2+y^2+1 & xy \\ xy & x^2+y^2+1 \end{pmatrix}.
$$

*Choose initial values $\psi$ and source terms $f$ such that the exact solution is*

$$
u = e^{-t}x(1-x)y(1-y),
$$

*where $\Gamma_N = \{(x,y) : y = 1\}$. In the example, we use triangular meshes and rectangular meshes.*

We list the errors and the numerical convergence orders in Tables 16-19. Tables 16-19 show that all convergence orders obtain the optimal order, consistent with our theoretical analysis.

TABLE 16. Numerical results by the $P_1$ CDG element with $\tau = h/2$ on triangular meshes in Example 5.6.

| 1/h | $\|\|\|u - u_h\|\|\|$ | order | $\|u - u_h\|$ | order |
|---|---|---|---|---|
| 4 | 1.2690E-01 | – | 2.0062E-03 | – |
| 8 | 7.2148E-02 | 0.8147 | 5.6540E-04 | 1.8271 |
| 16 | 3.8331E-02 | 0.9124 | 1.4889E-04 | 1.9250 |
| 32 | 1.9998E-02 | 0.9387 | 3.8701E-05 | 1.9438 |
| 64 | 9.9946E-03 | 1.0013 | 9.6199E-06 | 2.0083 |

## 6. Conclusion

This paper uses the conforming discontinuous Galerkin (CDG) finite element method to solve the second-order parabolic equation. Compared to the weak Galerkin (WG) finite element method, employing the average of the interior function in place of the boundary function reduces the number of degrees of freedom.

TABLE 17. Numerical results by the $P_2$ CDG element with $\tau = h^2$ on triangular meshes in Example 5.6.

| 1/h | $\|\|\|u - u_h\|\|\|$ | order | $\|u - u_h\|$ | order |
|---|---|---|---|---|
| 4 | 1.0855E-02 | – | 1.3421E-04 | – |
| 8 | 3.0288E-03 | 1.8415 | 1.9017E-05 | 2.8191 |
| 16 | 7.6566E-04 | 1.9840 | 2.3827E-06 | 2.9966 |
| 32 | 1.8176E-04 | 2.0747 | 2.7784E-07 | 3.1003 |
| 64 | 4.5424E-05 | 2.0013 | 3.4729E-08 | 3.0012 |

TABLE 18. Numerical results by the $P_1$ CDG element with $\tau = h$ on rectangular meshes in Example 5.6.

| 1/h | $\|\|\|u - u_h\|\|\|$ | order | $\|u - u_h\|$ | order |
|---|---|---|---|---|
| 4 | 1.1427E-01 | – | 2.1893E-03 | – |
| 8 | 6.1037E-02 | 0.9047 | 5.9557E-04 | 1.8782 |
| 16 | 2.7172E-02 | 1.1675 | 1.3549E-04 | 2.1361 |
| 32 | 1.2023E-02 | 1.1764 | 3.0438E-05 | 2.1542 |
| 64 | 5.3621E-03 | 1.1649 | 6.8002E-06 | 2.1622 |

TABLE 19. Numerical results by the $P_2$ CDG element with $\tau = h^2$ on rectangular meshes in Example 5.6.

| 1/h | $\|\|\|u - u_h\|\|\|$ | order | $\|u - u_h\|$ | order |
|---|---|---|---|---|
| 4 | 9.1664E-03 | – | 1.9417E-04 | – |
| 8 | 3.2712E-03 | 1.4865 | 2.8914E-05 | 2.7475 |
| 16 | 9.2522E-04 | 1.8220 | 3.7761E-06 | 2.9368 |
| 32 | 2.2585E-04 | 2.0344 | 4.4122E-07 | 3.0973 |
| 64 | 5.0689E-05 | 2.1556 | 4.7861E-08 | 3.2046 |

Eliminating the stabilizer further simplifies the numerical computations, decreasing the overall computational complexity. We have successfully devised a CDG method based on the backward Euler difference technique for the second-order parabolic equation. Additionally, we have rigorously derived the optimal order error estimates for the CDG numerical scheme. The validity and accuracy of the theory are confirmed through numerical experiments.

**Acknowledgments**

This research was supported by the National Natural Science Foundation of China (grant No. 11971198, 12001230, 12001232, 22341302), the National Key Research and Development Program of China (grant No. 2020YFA0713602, 2023YFA1008803), and the Key Laboratory of Symbolic Computation and Knowledge Engineering of Ministry of Education of China housed at Jilin University.

## References

[1] A. Al-Taweel, S. Hussain, and X. Wang. A stabilizer free weak Galerkin finite element method for parabolic equation. J. Comput. Appl. Math., 392 (2021), pp. Paper No. 113373, 12.

[2] A. Al-Taweel, S. Hussain, and X. Wang. Analysis of weak Galerkin finite element methods with supercloseness. Int. J. Numer. Anal. Model., 19 (2022), pp. 761–776.

[3] K. Eriksson, C. Johnson, and V. Thomée. Time discretization of parabolic problems by the discontinuous Galerkin method. RAIRO Modél. Math. Anal. Numér., 19 (1985), pp. 611–643.

[4] F. Gao and L. Mu. On $L^2$ error estimate for weak Galerkin finite element methods for parabolic problems. J. Comput. Math., 32 (2014), pp. 195–204.

[5] N. Kumar and B. Deka. Weak Galerkin finite element methods for parabolic problems with $L^2$ initial data. Int. J. Numer. Anal. Model., 20 (2023), pp. 199–228.

[6] J. Liu, S. Tavener, and Z. Wang. Lowest-order weak Galerkin finite element method for Darcy flow on convex polygonal meshes. SIAM J. Sci. Comput., 40 (2018), pp. B1229–B1252.

[7] J. Liu, S. Tavener, and Z. Wang. Penalty-free any-order weak Galerkin FEMs for elliptic problems on quadrilateral meshes. J. Sci. Comput., 83 (2020), pp. Paper No. 47, 19.

[8] X. Liu, Y. Zou, S. Chai, and H. Wang. Optimal convergence analysis of weak galerkin finite element methods for parabolic equations with lower regularity. Numer. Algorithms, 97 (2024), pp. 1323-1339.

[9] L. Mu, J. Wang, and X. Ye. Weak Galerkin finite element methods on polytopal meshes. Int. J. Numer. Anal. Model., 12 (2015), pp. 31–53.

[10] L. Mu, X. Ye, and S. Zhang. Development of pressure-robust discontinuous Galerkin finite element methods for the Stokes problem. J. Sci. Comput., 89 (2021), pp. Paper No. 26, 25.

[11] W. Qi and L. Song. Weak Galerkin method with implicit $\theta$-schemes for second-order parabolic problems. Appl. Math. Comput., 366 (2020), pp. 124731, 11.

[12] A. Quarteroni and A. Valli. Numerical approximation of partial differential equations. vol. 23, Springer Science & Business Media, 2008.

[13] B. Rivière. Discontinuous Galerkin methods for solving elliptic and parabolic equations. vol. 35 of Frontiers in Applied Mathematics, Society for Industrial and Applied Mathematics (SIAM), Philadelphia, PA, 2008. Theory and implementation.

[14] V. Thomée. Galerkin finite element methods for parabolic problems. vol. 25 of Springer Series in Computational Mathematics. Springer-Verlag, Berlin, second ed., 2006.

[15] G. Vacca and L. Beirão da Veiga. Virtual element methods for parabolic problems on polygonal meshes. Numer. Methods Partial Differential Equations, 31 (2015), pp. 2110–2134.

[16] C. Wang. A modified primal-dual weak Galerkin finite element method for second order elliptic equations in non-divergence form. Int. J. Numer. Anal. Model., 18 (2021), pp. 500–523.

[17] C. Wang. Low regularity primal-dual weak Galerkin finite element methods for ill-posed elliptic Cauchy problems. Int. J. Numer. Anal. Model., 19 (2022), pp. 33–51.

[18] J. Wang and X. Ye. A weak Galerkin finite element method for second-order elliptic problems. J. Comput. Appl. Math., 241 (2013), pp. 103–115.

[19] J. Wang and X. Ye. A weak Galerkin mixed finite element method for second order elliptic problems. Math. Comp., 83 (2014), pp. 2101–2126.

[20] J. Wang and X. Ye. A weak Galerkin finite element method for the stokes equations. Adv. Comput. Math., 42 (2016), pp. 155–174.

[21] J. Wang, X. Ye, and S. Zhang. A time-explicit weak Galerkin scheme for parabolic equations on polytopal partitions. J. Numer. Math., 31 (2023), pp. 125–135.

[22] X. Wang, Y. Liu, and Q. Zhai. The weak Galerkin finite element method for solving the time-dependent Stokes flow. Int. J. Numer. Anal. Model., 17 (2020), pp. 732–745.

[23] Y. Wang, F. Gao, and J. Cui. A conforming discontinuous Galerkin finite element method for elliptic interface problems. J. Comput. Appl. Math., 412 (2022), pp. Paper No. 114304, 12.

[24] Y. Wang, F. Gao, and J. Cui. A conforming discontinuous Galerkin finite element method for linear elasticity interface problems. J. Sci. Comput., 92 (2022), pp. Paper No. 9, 20.

[25] X. Ye and S. Zhang. A conforming discontinuous Galerkin finite element method. Int. J. Numer. Anal. Model., 17 (2020), pp. 110–117.

[26] X. Ye and S. Zhang. A conforming discontinuous Galerkin finite element method: Part II. Int. J. Numer. Anal. Model., 17 (2020), pp. 281–296.

[27] X. Ye and S. Zhang. A conforming discontinuous Galerkin finite element method: part III. Int. J. Numer. Anal. Model., 17 (2020), pp. 794–805.

[28] X. Ye and S. Zhang. A conforming discontinuous Galerkin finite element method for the Stokes problem on polytopal meshes. Internat. J. Numer. Methods Fluids, 93 (2021), pp. 1913–1928.

[29] X. Ye and S. Zhang. A $C^0$-conforming DG finite element method for biharmonic equations on triangle/tetrahedron. J. Numer. Math., 30 (2022), pp. 163–172.

[30] X. Ye and S. Zhang. A weak divergence CDG method for the biharmonic equation on triangular and tetrahedral meshes. Appl. Numer. Math., 178 (2022), pp. 155–165.

[31] Y. Zhang and D. Shi. Superconvergence of an $H^1$-Galerkin nonconforming mixed finite element method for a parabolic equation. Comput. Math. Appl., 66 (2013), pp. 2362–2375.

[32] J. Zhao, B. Zhang, and X. Zhu. The nonconforming virtual element method for parabolic problems. Appl. Numer. Math., 143 (2019), pp. 97–111.

[33] M. Zlámal. Finite element methods for parabolic equations. Math. Comp., 28 (1974), pp. 393–404.

Department of Mathematics, Jilin University, Changchun, China

*E-mail*: `huofc22@mails.jlu.edu.cn`, `sunyc21@mails.jlu.edu.cn`, `wujg22@mails.jlu.edu.cn` and `liyuanz20@mails.jlu.edu.cn`